

Constraining an R -parity violating supergravity model with the Higgs induced Majorana neutrino magnetic moments

Marek Gózdź*

*Department of Informatics, Maria Curie-Skłodowska University,
pl. Marii Curie-Skłodowskiej 5, 20-031 Lublin, Poland*

It is well known, that R -parity violating supersymmetric models predict a non-zero magnetic moment for neutrinos. In this work we study the Majorana neutrino transition magnetic moments within an RpV modified minimal supergravity model. Specifically, we discuss the contributions coming from the charged Higgs bosons, higgsinos, leptons, sleptons, charged gauge bosons, and charginos. We use the experimental results from the MUNU collaboration to restrict the model's parameter space. A comparison with two other types of contributions (only trilinear RpV couplings and trilinear plus neutrino–neutralino mixing) is also presented. We have found that the presently discussed processes dominate significantly, exceeding in some cases even the experimental limits.

PACS numbers: 11.30.Pb, 12.60.Jv, 14.60.Pq

Keywords: neutrino magnetic moment, supersymmetry, R-parity

I. INTRODUCTION

Neutrinos are one of the most mysterious particles known. They interact very weakly with matter, taking part only in the weak (and presumably gravitational) interactions. Due to mixing [1] their mass eigenstates and interaction eigenstates differ substantially, which gives rise to the generation lepton number violating oscillations [2]. They are also the lightest fermions ever observed – in fact the smallness of neutrino masses cannot be explained using the standard Higgs mechanism [3]. All this indicates, that neutrinos are a window to some new physics beyond the standard model.

The possible electromagnetic properties of neutrinos in the form of an induced magnetic moment are particularly interesting, since the electromagnetic interactions are much easier to control in any precise measurement. This problem has been studied in the standard model [4, 5] and its extensions. In Ref. [6] the magnetic moments have been reviewed in models with spontaneously broken lepton number. A lot of work has been devoted to discuss the neutrino masses in the R -parity violating (RpV) supersymmetry [7–14]. In these models, the neutrino mass is generated mostly at the one-loop level through an RpV loop containing in the simplest version a particle–sparticle pair (lepton–slepton or quark–squark). The approach usually used in the literature assumed no mixing among particles, and some average common value for the masses of the superparticles at low energies. In Ref. [15] a basis independent classification of various diagrams leading to Majorana neutrino masses has been presented. The study of neutrino masses can be directly extended to the magnetic moment case by introducing an interaction with an external photon.

A more systematic approach to the calculations of the

magnetic moments has been presented in our previous works [13, 16–18]. The SUGRA model has been used to calculate masses and magnetic moments in Ref. [16]. The contribution coming from neutrino–neutralino mixing has been discussed in Ref. [17], while the contribution from generic diagrams with two mass insertions on the internal lines was presented in [13]. Calculations within the gauge-mediated model were performed in [18]. We have studied the Majorana neutrino masses and transition magnetic moments using exact analytic formulas and up-to-date experimental data concerning neutrino oscillations and the non-observability of the neutrinoless double beta decay ($0\nu 2\beta$). Our numerical procedure rested upon the assumption that most of the free parameters of the supersymmetric model unify in certain way at the GUT scale $m_{\text{GUT}} \sim 1.2 \times 10^{16}$ GeV. This allows to reduce the number of free parameters to few, and calculate the rest by performing renormalization group evolution. Such approach gives a much more convincing picture of the low energy spectrum than just assessing the running masses of the superparticles. We have also demonstrated the influence of the mixing among squarks and quarks on the results. The evident weak point of our approach was the lack of knowledge of the trilinear coupling constants, which forced us to use additional source of constraints (neutrino oscillations, $0\nu 2\beta$ decay).

In this paper we study the Majorana neutrino transition magnetic moments generated in the R -parity violating modified minimal supergravity model. This model, based on the Ref. [19], takes into account the full dependence of the renormalization group equations (RGE) on the RpV couplings and their soft SUSY breaking versions. All these couplings have been incorporated in the unification scheme, so, within this assumption, the whole model can be calculated numerically. No other input, in particular experimental data, is needed. We concentrate on the contributions coming from the charged Higgs bosons, charged higgsinos, charged gauge bosons, charginos, leptons, and sleptons. The neutral particles, like the neutral components of the Higgs bosons, neu-

*Electronic address: mgozdz@kft.umcs.lublin.pl

tralinos and sneutrinos will contribute to the neutrino mass, but will not contribute to the magnetic moment, and as such will not be discussed here.

The paper is organized as follows. After the introduction, in Sect. II the minimal supersymmetric standard model with R -parity violation and supersymmetry broken by the gravitational interactions is presented. Sect. III is devoted to the technical problems of handling the free parameters and calculating the coupling constants in the Higgs sector during the electroweak symmetry breaking. The Majorana neutrino transition magnetic moments, and the interesting for us contributions to this quantity are discussed in Sect. IV. At the end numerical results are presented.

II. R -PARITY VIOLATING SUGRA

The minimal supersymmetric standard model (MSSM) [21, 22] is the minimal extension of the standard model (SM) of particles and interactions, which introduces supersymmetry (SUSY). In short, for each particle there is a new superpartner (fermionic for bosons and bosonic for fermions) so that the number of fermionic and bosonic degrees of freedom in the MSSM are equal. The one additional multiplet, not present in the SM, is a second Higgs doublet needed to cancel the gauge anomalies and to give masses to both the up and down components of the $SU(2)$ doublets. This version of the model preserves the so-called R -parity, which is a multiplicative quantum number defined as $R = (-1)^{2S+3(B-L)}$, S being the spin of the particle, B the baryon, and L the lepton number. One easily sees, that $R = +1$ for ordinary standard model particles, while $R = -1$ for the supersymmetric partners. Preserving R not only gives the baryon and lepton number conservations but also forbids decays of SUSY particles into SM particles, leaving the lightest SUSY particle stable.

The problem of the lepton and baryon number conservation is still disputable. On one hand, our observations suggest, that both B and L are conserved quantum numbers. Especially strong limits on B violation come from the non-observation of the proton decay. On the other hand, in the SM not only the total lepton number but also generation lepton numbers L_e , L_μ , and L_τ are conserved, and this rule has been proven wrong after the discovery of neutrino oscillations. From the theoretical point of view, there is no underlying symmetry or mechanism, which supports conservation of B and L ,

which might suggest that it is only an accidental (not exact) symmetry present in the low-energy regime. It is generally expected, that the higher-energy extensions of the SM will not preserve at least the lepton number (the proton stability must still hold). Such models based on supersymmetry introduce new interactions, or in fact do not rule out certain terms, that should be present in the superpotential, which violate R -parity [23–27]. They have a much richer phenomenology and predict lots of new phenomena, like the lepton number violating neutrinoless double beta decay, RpV loop-corrected neutrino mass and magnetic moment, and others.

We work within the slightly modified model described in details in Ref. [19]. It is defined by the following R -parity conserving and R -parity violating parts of the superpotential

$$W = W_{\text{RpC}} + W_{\text{RpV}}, \quad (1)$$

where

$$W_{\text{RpC}} = \epsilon_{ab} \left[(\mathbf{Y}_E)_{ij} L_i^a H_d^b \bar{E}_j + (\mathbf{Y}_D)_{ij} Q_i^{ax} H_d^b \bar{D}_{jx} + (\mathbf{Y}_U)_{ij} Q_i^{ax} H_u^b \bar{U}_{jx} - \mu H_d^a H_u^b \right], \quad (2)$$

$$W_{\text{RpV}} = \epsilon_{ab} \left[\frac{1}{2} (\mathbf{\Lambda}_{E^k})_{ij} L_i^a L_j^b \bar{E}_k + (\mathbf{\Lambda}_{D^k})_{ij} L_i^a Q_j^{xb} \bar{D}_{kx} \right] + \frac{1}{2} \epsilon_{xyz} (\mathbf{\Lambda}_{U^i})_{jk} \bar{U}_i^x \bar{D}_j^y \bar{D}_k^z - \epsilon_{ab} \kappa^i L_i^a H_u^b. \quad (3)$$

Here \mathbf{Y} 's are the 3×3 trilinear Yukawa-like couplings, μ the bilinear Higgs coupling, and $\mathbf{\Lambda}$ and κ^i represent the magnitudes of the R -parity violating trilinear and bilinear terms. L and Q denote the $SU(2)$ left-handed doublets, while \bar{E} , \bar{U} and \bar{D} are the right-handed lepton, up-quark and down-quark $SU(2)$ singlets, respectively. H_d and H_u mean two Higgs doublets. We have introduced color indices $x, y, z = 1, 2, 3$, generation indices $i, j, k = 1, 2, 3 = e, \mu, \tau$ and the $SU(2)$ gauge indices $a, b = 1, 2$. Finally, ϵ_{ab} and ϵ_{xyz} with $\epsilon_{12} = \epsilon_{123} = 1$ are the totally antisymmetric tensor densities.

The supersymmetry is not observed in the regime of energies accessible to our experiments. Therefore it must be broken at some point. A convenient method to take this fact into account is to introduce explicit terms, which break supersymmetry in a soft way, *ie.*, they do not suffer from ultraviolet divergencies. We add them in the form of a scalar Lagrangian [19],

$$\begin{aligned}
-\mathcal{L} = & m_{H_d}^2 h_d^\dagger h_d + m_{H_u}^2 h_u^\dagger h_u + l^\dagger (\mathbf{m}_L^2) l + l_i^\dagger (\mathbf{m}_{L_i H_d}^2) h_d + h_d^\dagger (\mathbf{m}_{H_d L_i}^2) l_i + q^\dagger (\mathbf{m}_Q^2) q + e (\mathbf{m}_E^2) e^\dagger + d (\mathbf{m}_D^2) d^\dagger + u (\mathbf{m}_U^2) u^\dagger \\
& + \frac{1}{2} \left(M_1 \tilde{B}^\dagger \tilde{B} + M_2 \tilde{W}_i^\dagger \tilde{W}^i + M_3 \tilde{g}_\alpha^\dagger \tilde{g}^\alpha + \text{h.c.} \right) \\
& + [(\mathbf{A}_E)_{ij} l_i h_d e_j + (\mathbf{A}_D)_{ij} q_i h_d d_j + (\mathbf{A}_U)_{ij} q_i h_u u_j - B h_d h_u \\
& + (\mathbf{A}_{E^k})_{ij} l_i l_j e_k + (\mathbf{A}_{D^k})_{ij} l_i q_j d_k + (\mathbf{A}_{U^i})_{jk} u_i d_j d_k - D_i l_i h_u + \text{h.c.}],
\end{aligned} \quad (4)$$

where the lower case letter denotes the scalar part of the respective superfield. M_i are the gaugino masses, and \mathbf{A} (B , D_i) are the soft supersymmetry breaking equivalents of the trilinear (bilinear) couplings from the superpotential.

III. FREE PARAMETERS AND THE LOW-ENERGY SPECTRUM

The main problem of most supersymmetric models is their large number of free parameters. Therefore additional constraints are usually imposed, which introduce certain relations among them, effectively reducing their number. It is a well known fact, that the RGE equations for the gauge coupling constants lead in the MSSM model to their unification at energy $m_{\text{GUT}} \approx 1.2 \times 10^{16}$ GeV. This feature is absent in the SM, although suggested by the extrapolation of the LEP1 data. It may therefore seem natural to assume also certain type of unification of other parameters. Let us introduce at m_{GUT} :

- the common mass of all the scalars m_0 ,
- the common mass of all the fermions $m_{1/2}$,
- the common proportionality factor A_0 for the soft SUSY breaking couplings

$$\begin{aligned} \mathbf{A}_{U,D,E} &= A_0 \mathbf{Y}_{U,D,E}, \\ \mathbf{A}_{U^i,D^i,E^i} &= A_0 \mathbf{Y}_{U,D,E} \quad (i = 1, 2, 3). \end{aligned} \quad (5)$$

This scheme of unification follows the mSUGRA assumptions with the exception that we do not assume the total universality of the \mathbf{A} couplings, but vary them keeping them proportional to the Yukawa \mathbf{Y} coupling constants at the unification scale. As a free parameter remains also the ratio of the Higgs vacuum expectation values, $\tan \beta = v_u/v_d$, and the sign of the μ coupling constant, $\text{sgn}(\mu)$. The sixth free parameter in our considerations is the initial value of the $\mathbf{\Lambda}$'s at m_Z , Λ_0 . We leave this value free and investigate its influence on the results. The idea is that we want to have $\mathbf{\Lambda}$'s non-zero and contributing from the beginning to the RGE running of other parameters. In this way, Λ_0 controls the amount of R -parity violation in the low energy regime. Notice, that $\mathbf{\Lambda}$'s will not unify at m_{GUT} , although their RGE running is almost flat (cf. Fig. 1 in Ref. [20]).

The procedure of obtaining the low energy spectrum of the model involves few renormalization group runnings between the low (m_Z) and high energy scale (m_{GUT}), and between m_Z and the scale at which the electroweak symmetry breaking occurs, which is defined by the top

squark mass eigenstates as

$$q_{\text{min}} = \sqrt{m_{\tilde{t}_1} m_{\tilde{t}_2}}. \quad (6)$$

At this scale the radiative corrections to the Higgs potential coming from the squarks are minimal. We start by fixing the Yukawa couplings at m_Z using the quark and lepton mass matrices $M_{U,D,E}$

$$\begin{aligned} M_U &= v_u \mathbf{S}_{U_R} \mathbf{Y}_U^T \mathbf{S}_{U_L}^\dagger, \\ M_D &= v_d \mathbf{S}_{D_R} \mathbf{Y}_D^T \mathbf{S}_{D_L}^\dagger, \\ M_E &= v_d \mathbf{S}_{E_R} \mathbf{Y}_E^T \mathbf{S}_{E_L}^\dagger, \end{aligned} \quad (7)$$

where \mathbf{S} matrices perform diagonalization so that one obtains eigenstates in the mass representation. The Yukawa-like RpV couplings at m_Z are all set to

$$\mathbf{\Lambda} = \Lambda_0 \mathbf{1}, \quad (8)$$

$\mathbf{1}$ being a 3×3 unit matrix. Next, we evolve the gauge and Yukawa couplings from m_Z to the unification scale. During this running we turn off the Higgs sector, $\mu = \kappa_i = B = D_i = 0$, and set the sneutrino vev's $v_i = 0$. These parameters will be calculated later.

At m_{GUT} we impose the GUT conditions as described above, ie., we set the masses of all the scalars to m_0 , of all the fermions to $m_{1/2}$, and the soft breaking couplings to $A_0 \mathbf{Y}$. The Yukawa couplings \mathbf{Y} 's are left unchanged in order to reproduce correctly the masses of leptons and quarks when evolved down to m_Z . So are the $\mathbf{\Lambda}$'s, which are free parameters here. We evolve all the running parameters, coupling constants and masses, down, and find the best scale for minimizing the scalar potential Eq. (6) and at this scale calculate $\mu = \text{sgn}(\mu) \sqrt{|\mu|^2}$ and B using [19]

$$|\mu|^2 = \frac{m_{H_d}^2 - m_{H_u}^2 \tan^2 \beta}{\tan^2 \beta - 1} - \frac{M_Z^2}{2}, \quad (9)$$

$$B = \frac{\sin 2\beta}{2} (m_{H_d}^2 - m_{H_u}^2 + 2|\mu|^2). \quad (10)$$

Running all the parameters down $q_{\text{min}} \rightarrow m_Z$ non-zero μ and B generate non-zero κ_i and D_i . These are used as the starting values to the second long run. Next, we perform once again the RGE running up to the m_{GUT} scale, but now with all the Higgs parameters contributing to the running. We impose GUT conditions, go down, calculate the new q_{min} scale and once again evaluate the corrected Higgs parameters, this time together with the sneutrino vev's, according to

$$|\mu|^2 = \frac{1}{\tan^2 \beta - 1} \left\{ \left[m_{H_d}^2 + \mathbf{m}_{L_i H_d}^2 \frac{v_i}{v_d} + \kappa_i^* \mu \frac{v_i}{v_d} \right] - \left[m_{H_u}^2 + |\kappa_i|^2 - \frac{1}{2} (g^2 + g_2^2) v_i^2 - D_i \frac{v_i}{v_u} \right] \tan^2 \beta \right\} - \frac{M_Z^2}{2}, \quad (11)$$

$$B = \frac{\sin 2\beta}{2} \left[(m_{H_d}^2 - m_{H_u}^2 + 2|\mu|^2 + |\kappa_i|^2) + (\mathbf{m}_{L_i H_d}^2 + \kappa_i^* \mu) \frac{v_i}{v_d} - D_i \frac{v_i}{v_u} \right], \quad (12)$$

$$\begin{aligned} v_1[(\mathbf{m}_L^2)_{11} + |\kappa_1|^2 + D'] + v_2[(\mathbf{m}_L^2)_{21} + \kappa_1 \kappa_2^*] + v_3[(\mathbf{m}_L^2)_{31} + \kappa_1 \kappa_3^*] &= -[\mathbf{m}_{H_d L_1}^2 + \mu^* \kappa_1] v_d + D_1 v_u, \\ v_1[(\mathbf{m}_L^2)_{12} + \kappa_2 \kappa_1^*] + v_2[(\mathbf{m}_L^2)_{22} + |\kappa_2|^2 + D'] + v_3[(\mathbf{m}_L^2)_{32} + \kappa_2 \kappa_3^*] &= -[\mathbf{m}_{H_d L_2}^2 + \mu^* \kappa_2] v_d + D_2 v_u, \\ v_1[(\mathbf{m}_L^2)_{13} + \kappa_3 \kappa_1^*] + v_2[(\mathbf{m}_L^2)_{23} + \kappa_3 \kappa_2^*] + v_3[(\mathbf{m}_L^2)_{33} + |\kappa_3|^2 + D'] &= -[\mathbf{m}_{H_d L_3}^2 + \mu^* \kappa_3] v_d + D_3 v_u, \end{aligned} \quad (13)$$

where $D' = M_Z^2 \frac{\cos 2\beta}{2} + (g^2 + g_2^2) \frac{\sin^2 \beta}{2} (v^2 - v_u^2 - v_d^2)$. The tadpole equations (13) can be easily solved and we get for the sneutrino vev's

$$v_i = \frac{\det W_i}{\det W}, \quad i = 1, 2, 3, \quad (14)$$

where

$$W = \begin{pmatrix} (\mathbf{m}_L^2)_{11} + |\kappa_1|^2 + D' & (\mathbf{m}_L^2)_{21} + \kappa_1 \kappa_2^* & (\mathbf{m}_L^2)_{31} + \kappa_1 \kappa_3^* \\ (\mathbf{m}_L^2)_{12} + \kappa_2 \kappa_1^* & (\mathbf{m}_L^2)_{22} + |\kappa_2|^2 + D' & (\mathbf{m}_L^2)_{32} + \kappa_2 \kappa_3^* \\ (\mathbf{m}_L^2)_{13} + \kappa_3 \kappa_1^* & (\mathbf{m}_L^2)_{23} + \kappa_3 \kappa_2^* & (\mathbf{m}_L^2)_{33} + |\kappa_3|^2 + D' \end{pmatrix}, \quad (15)$$

and W_i can be obtained from W by replacing the i -th column with

$$\begin{pmatrix} -[\mathbf{m}_{H_d L_1}^2 + \mu^* \kappa_1] v_d + D_1 v_u \\ -[\mathbf{m}_{H_d L_2}^2 + \mu^* \kappa_2] v_d + D_2 v_u \\ -[\mathbf{m}_{H_d L_3}^2 + \mu^* \kappa_3] v_d + D_3 v_u \end{pmatrix}. \quad (16)$$

The newly obtained v_i 's are incorporated in the scheme in the following way:

$$v_u = \sin \beta \sqrt{v^2 - (v_1^2 + v_2^2 + v_3^2)}, \quad (17)$$

$$v_d = \cos \beta \sqrt{v^2 - (v_1^2 + v_2^2 + v_3^2)}, \quad (18)$$

$v^2 = (246 \text{ GeV})^2$, which preserves the definition of the $\tan \beta$ and $v^2 = v_u^2 + v_d^2 + v_1^2 + v_2^2 + v_3^2$. Notice, that in this model sneutrino vev's contribute to the mass of the Z and W bosons. The equations (11)–(13) are solved subsequently until convergence and self-consistency of the results is obtained. In practice three iterations turned out to be enough. After this procedure we add also the dominant radiative corrections [28], and get back to the m_Z scale to obtain the mass spectrum of the model.

IV. NEUTRINO MAGNETIC MOMENTS

It is well known that in the RpV supersymmetric models only one neutrino gains mass after the diagonalization of the neutrino–neutralino mass matrix. The remaining contributions come from the sneutrino vev's at the tree level and from the one-loop processes. The main one-loop mechanism involves decomposing a Majorana neutrino–neutrino vertex into a particle–sparticle loop, which basically is either the quark–squark, or the (charged) lepton–slepton loop. These contributions will be proportional to some functions of the masses of the particles and $(\mathbf{\Lambda}_D)^2$

or $(\mathbf{\Lambda}_E)^2$. Detailed discussions can be found, e.g., in Refs. [7–12, 15].

Neutrinos are neutral particles and as such cannot interact with photons. However, this interaction is possible through the one-loop mechanism, in which charged particles appear in the loop. Therefore, an effective neutrino magnetic moment may be generated. Due to the CPT theorem, Majorana neutrinos cannot have diagonal magnetic moments, which act between the same flavours of neutrinos, but they may have the off-diagonal transition magnetic moments [4]. To be more precise, the transition Majorana magnetic moment acts between ν_{iL} and ν_{jL}^c chiral components of Majorana neutrinos, assuming gauge theory with only left-handed neutrinos. As a consequence it violates the total lepton number by two units ($\Delta L = 2$), and can be discussed provided that R -parity violation occurs. The effective Hamiltonian takes the form

$$H_{\text{eff}}^M = \frac{1}{2} \mu_{ij} \bar{\nu}_{iL} \sigma^{\alpha\beta} \nu_{jL}^c F_{\beta\alpha} + \text{h.c.} \quad (19)$$

The contributing Feynman diagrams are presented on Fig. 1. We will evaluate the amplitudes of these processes in the interaction basis, in which the vertex coupling constants are known directly from the mixing matrices. However, one has to take into account, that the propagators of particles travelling inside the loop must be written for their mass eigenstates. This can be done using the mixed-propagator formalism [29]. Assume the following relation between the mass (j) and interaction

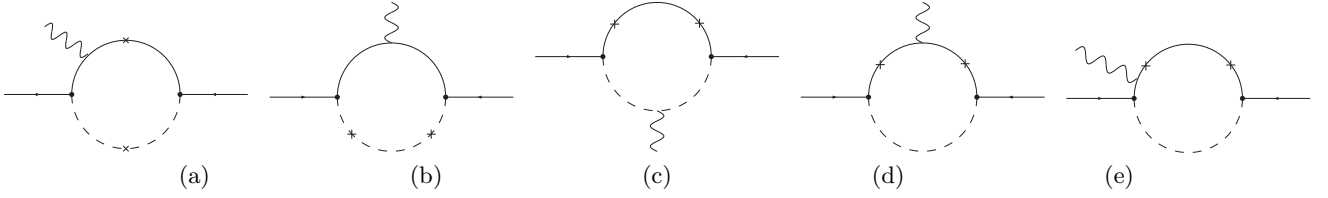


FIG. 1: Feynman diagrams with two mass insertions inside the loop contributing to the Majorana neutrino transition magnetic moments.

(α) eigenstates of some particle,

$$\Phi_\alpha = \sum_j V_{\alpha j} \Phi_j. \quad (20)$$

Then, the amplitude in the weak basis can be written in terms of the Green function and expanded in the mass basis

$$\mathcal{A}_\alpha \sim G_{\Phi_\alpha} = \sum_j V_{\alpha j} G_j V_{j\alpha}^\dagger, \quad (21)$$

so the flavour changing amplitude may be written as

$$\mathcal{A}(\alpha \rightarrow \beta) = \sum_j V_{\beta j} \mathcal{A}_j V_{j\alpha}^\dagger. \quad (22)$$

A more detailed derivation and discussion of this result can be found in Sect. 4.2 of Ref. [29].

The matrix V is obtained during the diagonalization procedure of the mixing matrices and its columns are the eigenvectors of the mixing matrix. The magnetic moment will consist of the product of numerical constants, coupling constants, and the function \mathcal{I} describing the loop

integral, so it may be written in a general form as

$$\mu_\nu = \left[\sum N_c C_1 C_2 X_1 X_2 Q \mathcal{I} \right] 2m_e \mu_B, \quad (23)$$

where N_c is the color index ($=3$ for quarks and squarks, $=1$ otherwise), $C_{1,2}$ are the trilinear coupling constants, $X_{1,2}$ are the mass insertions residing inside the loop, Q is the charge of the particle the photon is attached to (in units of the elementary charge), m_e is the electron mass ($2m_e \approx 10^{-3}$ GeV), and μ_B the Bohr magneton. The sum runs over all mass eigenstates which form every mixed particle present in the loop.

The masses and couplings in our approach are calculated from the boundary conditions at the m_Z and m_{GUT} scales (see Sect. III). The loop integrals \mathcal{I} can be derived analytically using standard techniques of integration in the Minkowski space. Denoting by f_1, f_2, \dots and b_1, b_2, \dots the fermions and bosons which appear in the loop, and by $m_{f,b}$ their respective masses, the loop integrals for diagrams (a)–(e) depicted on Fig. 1 read

$$\mathcal{I}^{(a)} = m_{f_1} m_{f_2} \mathcal{F}_3(f_1, f_2, b_1, b_2) + \mathcal{F}_4(f_1, f_2, b_1, b_2) + m_{f_1} m_{f_2} \mathcal{F}_3(f_2, f_1, b_1, b_2) + \mathcal{F}_4(f_2, f_1, b_1, b_2), \quad (24)$$

$$\mathcal{I}^{(b)} = m_{f_1} \mathcal{F}_3(f_1, b_1, b_2, b_3), \quad (25)$$

$$\mathcal{I}^{(c)} = 4 \mathcal{F}_4(b_1, f_1, f_2, f_3), \quad (26)$$

$$\mathcal{I}^{(d)} = m_{f_1} m_{f_2} (m_{f_2} + m_{f_3}) \mathcal{F}_3(f_2, f_1, f_3, b_1) + (2m_{f_1} + 3m_{f_2} + m_{f_3}) \mathcal{F}_4(f_2, f_1, f_3, b_1), \quad (27)$$

$$\begin{aligned} \mathcal{I}^{(e)} = & m_{f_1} (m_{f_1} m_{f_2} + m_{f_2} m_{f_3} + m_{f_3} m_{f_1}) \mathcal{F}_3(f_1, f_2, f_3, b_1) + (5m_{f_1} + 2m_{f_2} + 2m_{f_3}) \mathcal{F}_4(f_1, f_2, f_3, b_1) \\ & + m_{f_3} (m_{f_1} m_{f_2} + m_{f_2} m_{f_3} + m_{f_3} m_{f_1}) \mathcal{F}_3(f_3, f_1, f_2, b_1) + (5m_{f_3} + 2m_{f_2} + 2m_{f_1}) \mathcal{F}_4(f_3, f_1, f_2, b_1), \end{aligned} \quad (28)$$

where the functions $\mathcal{F}_{3,4}$ are given by

$$\begin{aligned} (16\pi^2) \mathcal{F}_3(a, b, c, d) &= (16\pi^2) \int_{-\infty}^{\infty} \frac{d^4 k}{(2\pi)^4} \frac{1}{(k^2 - m_a^2)^2 (k^2 - m_b^2) (k^2 - m_c^2) (k^2 - m_d^2)} \\ &= \frac{m_a^2 \log(m_a^2) \left(\frac{1}{m_a^2 - m_b^2} + \frac{1}{m_a^2 - m_c^2} + \frac{1}{m_a^2 - m_d^2} - 1 \right) - 1}{(m_a^2 - m_b^2)(m_a^2 - m_c^2)(m_a^2 - m_d^2)} - \frac{m_b^2 \log(m_b^2)}{(m_b^2 - m_a^2)(m_b^2 - m_c^2)(m_b^2 - m_d^2)} \\ &\quad - \frac{m_c^2 \log(m_c^2)}{(m_c^2 - m_a^2)(m_c^2 - m_b^2)(m_c^2 - m_d^2)} - \frac{m_d^2 \log(m_d^2)}{(m_d^2 - m_a^2)(m_d^2 - m_b^2)(m_d^2 - m_c^2)}, \end{aligned} \quad (29)$$

$$(16\pi^2) \mathcal{F}_4(a, b, c, d) = (16\pi^2) \int_{-\infty}^{\infty} \frac{d^4 k}{(2\pi)^4} \frac{k^2}{(k^2 - m_a^2)^2 (k^2 - m_b^2) (k^2 - m_c^2) (k^2 - m_d^2)}$$

$$\begin{aligned}
&= \frac{m_a^4 \log(m_a^2) \left(\frac{1}{m_a^2 - m_b^2} + \frac{1}{m_a^2 - m_c^2} + \frac{1}{m_a^2 - m_d^2} - 2 \right) - 1}{(m_a^2 - m_b^2)(m_a^2 - m_c^2)(m_a^2 - m_d^2)} - \frac{m_b^4 \log(m_b^2)}{(m_b^2 - m_a^2)(m_b^2 - m_c^2)(m_b^2 - m_d^2)} \\
&- \frac{m_c^4 \log(m_c^2)}{(m_c^2 - m_a^2)(m_c^2 - m_b^2)(m_c^2 - m_d^2)} - \frac{m_d^4 \log(m_d^2)}{(m_d^2 - m_a^2)(m_d^2 - m_b^2)(m_d^2 - m_c^2)}. \tag{30}
\end{aligned}$$

We have kept denotations from Ref. [13]. Please notice also that a typo has been corrected in Eq. (25), and new terms appeared in Eqs. (24) and (28).

V. RESULTS

In order to contribute to the neutrino magnetic moment, the loop must contain charged particles. The quarks–squarks and leptons–sleptons have already been discussed elsewhere (see Sect. I). The discussion on the bilinear insertions on the neutrino lines, possible due to the neutrino–neutralino mixing, can be found in Refs. [14, 17]. In this work we have focused on the charged Higgs–sleptons and the leptons–charginos interaction eigenstates.

Altogether we have identified 45 diagrams of the forms given on Fig. 1 containing the particles in question. The way of obtaining them is a straightforward but rather tedious task, and we have used a computer program to match all possible vertices and internal lines to the given patterns. The trilinear vertices can be constructed directly from the superpotential (1), and the possible bilinear mass insertions are defined by the mixing matrices, as given in Ref. [19].

A few conditions must have been met for the result to be accepted. First of all, during the RGE evolution some of the particles may get negative mass parameters squared. Such tachyonic behaviour resulted in immediate rejecting of the given input parameters. Also, finite values for the Yukawa couplings, which tend to ‘explode’ for too low or too high values of the $\tan\beta$, were required. When analyzing the results, we have rejected points, for which the masses of the superparticles were too low. The mass limits we have used were taken from the Particle Data Group report [30], and they read: $m_{\tilde{\chi}_1^0} > 46$ GeV, $m_{\tilde{\chi}_2^0} > 62$ GeV, $m_{\tilde{\chi}_3^0} > 100$ GeV, $m_{\tilde{\chi}_4^0} > 116$ GeV, $m_{\tilde{\chi}_1^\pm} > 94$ GeV, $m_{\tilde{\chi}_2^\pm} > 94$ GeV, $m_{\tilde{e}} > 107$ GeV, $m_{\tilde{\mu}} > 94$ GeV, $m_{\tilde{\tau}} > 82$ GeV, $m_{\tilde{q}} > 379$ GeV, $m_{\tilde{g}} > 308$ GeV. This is by far the conservative choice of constraints. The new results from the LHC projects push the quoted above limits to higher values, closer to the 1 TeV range. We do not use them here for various reasons. Firstly, most of the results are still marked as preliminary, and more careful data analysis is being performed right now. Also, the LHC data are interpreted within the simplest SUSY models, with many additional assumptions, like the absence of R -parity violation, and equality of the gluino and squark masses. These assumptions are not true in the model used here.

A. Constraining the model’s parameter space with the magnetic moments

There are different assessments and constraints put on the neutrino magnetic moment. Analyzing the impact of the solar neutrino data on the neutrino spin-flavour-precession mechanism, the authors of Ref. [31] have found a model-dependent upper value for the magnetic moment to be $\text{few} \times 10^{-12} \mu_B$. On the other hand, direct searches in the MUNU experiment resulted in the upper limit to be $9 \times 10^{-11} \mu_B$ [32]. In this paper we adopt a conservative limit and reject points, for which $\mu_\nu \geq 10^{-10} \mu_B$. A more strict approach would result in a substantially narrower parameter space of the model.

The results are presented on Figs. 2–9, for $\mu > 0$, $\Lambda_0 = 10^{-4}$, $A_0 = 200 - 1000$ GeV in steps of 100, $m_{0,1/2} = 200 - 1000$ GeV in steps of 20, and $\tan\beta = 5 - 40$ in steps of 5. Each point represents a valid set of input parameters, which results in a physically accepted low energy spectrum. Each figure represents a fixed $\tan\beta$, and panels read in rows from left to right correspond to A_0 taking values 200 GeV, 300 GeV, \dots , 1000 GeV.

In general, there is no global regularity in these results. Certain regions are excluded due to unaccepted values of the masses. The excluded stripes, visible in several of the panels, come from too high values of μ_ν . Starting from $\tan\beta = 15$, a parabolic-like shape, whose position depends on the A_0 parameter, appears. It starts to be visible for $A_0 = 400$ GeV and crosses the $m_0 - m_{1/2}$ plane with increasing A_0 . [We are not sure about the origin of this ‘stability line’. As a side remark we add, that it appeared also in our analysis of the masses of the lightest Higgs bosons h^0 in the context of the CDF-D0 discovery [33]. Constructing similar plots, but using the condition, that $120 \text{ GeV} < m_{h^0} < 140 \text{ GeV}$, we have observed very similar parabolas.] We notice also, that for $\tan\beta = 40$ the points look totally random, which shows that the model breaks down in this region due to too high values of the Yukawa couplings.

B. Λ_0 dependence

Another interesting problem is how the initial value of the RpV couplings at m_Z , represented by a common parameter Λ_0 , influences the results. We have chosen to check this relation for a few specific sets of parameters. For this, the Snowmass SUSY benchmark points [34] were used. The dependence of the resulting contribution to the transition magnetic moments have been calculated for

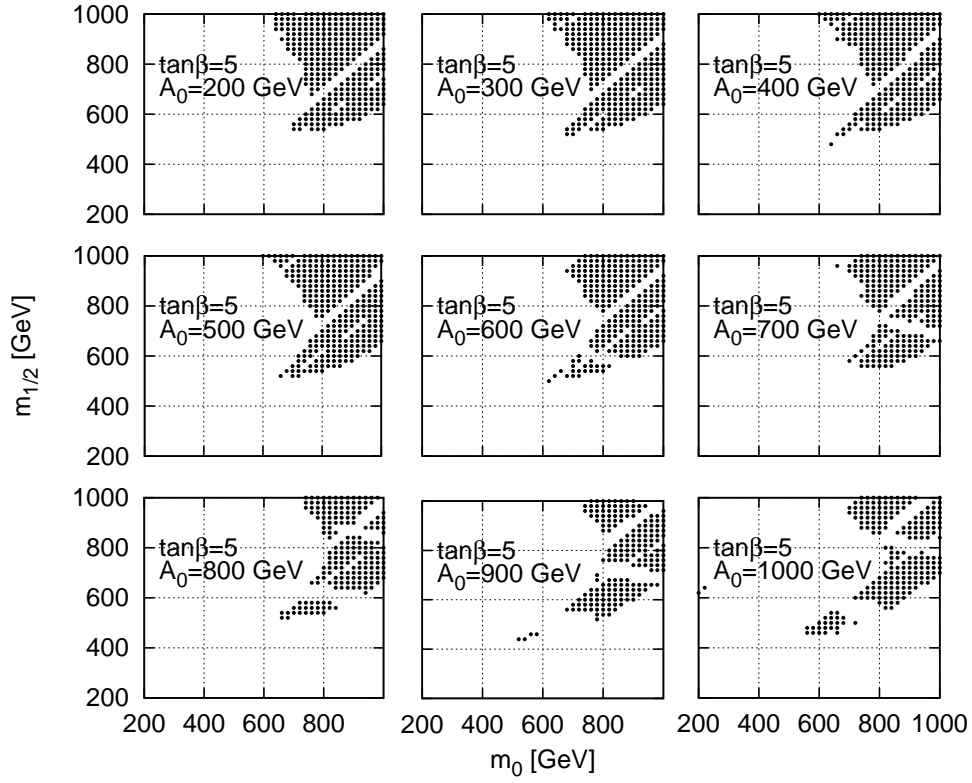


FIG. 2: Allowed parameter space of the model for $\tan\beta = 5$ and $\mu > 0$. The parameter A_0 changes as indicated on the panels.

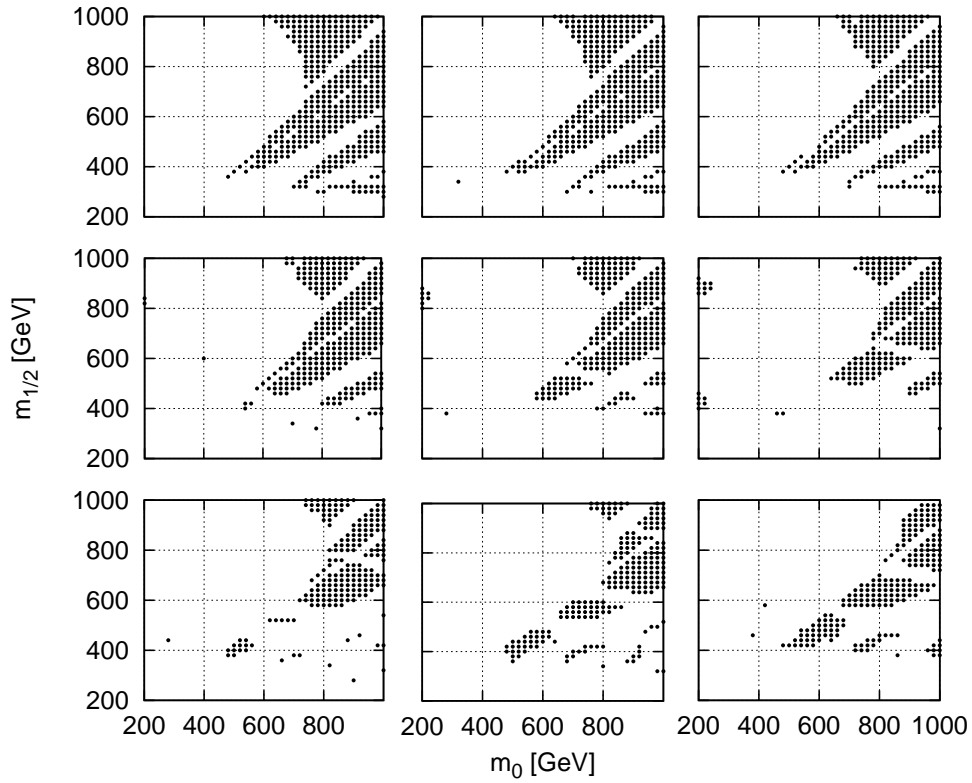


FIG. 3: Like Fig. 2 but for $\tan\beta = 10$.

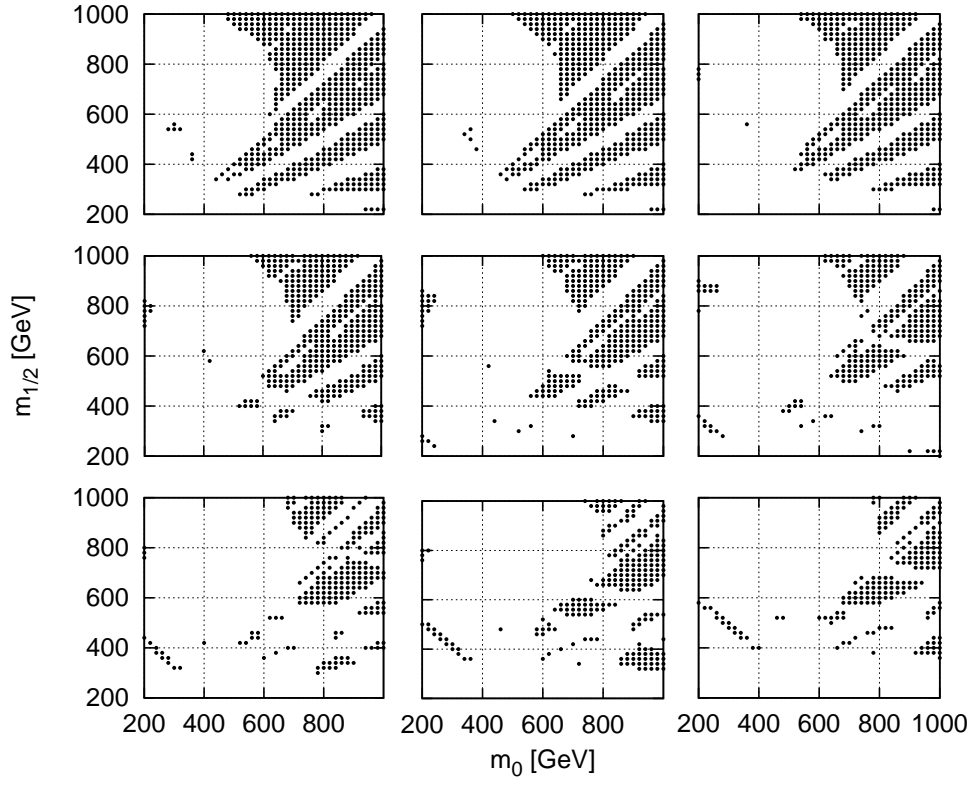


FIG. 4: Like Fig. 2 but for $\tan\beta = 15$.

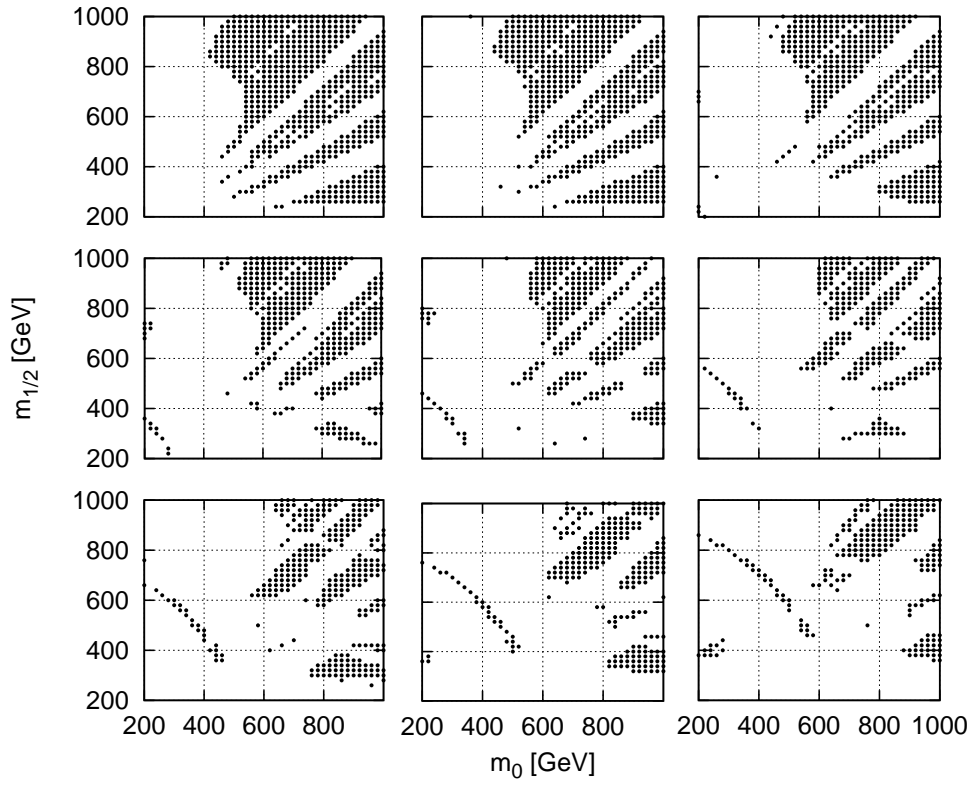


FIG. 5: Like Fig. 2 but for $\tan\beta = 20$.

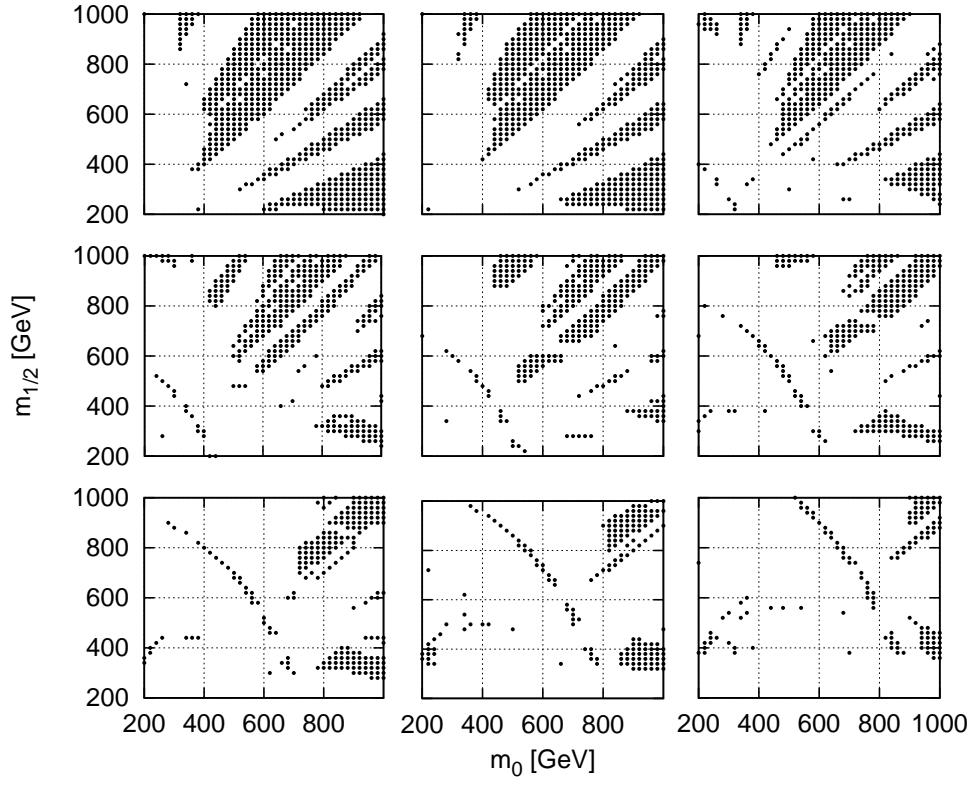


FIG. 6: Like Fig. 2 but for $\tan \beta = 25$.

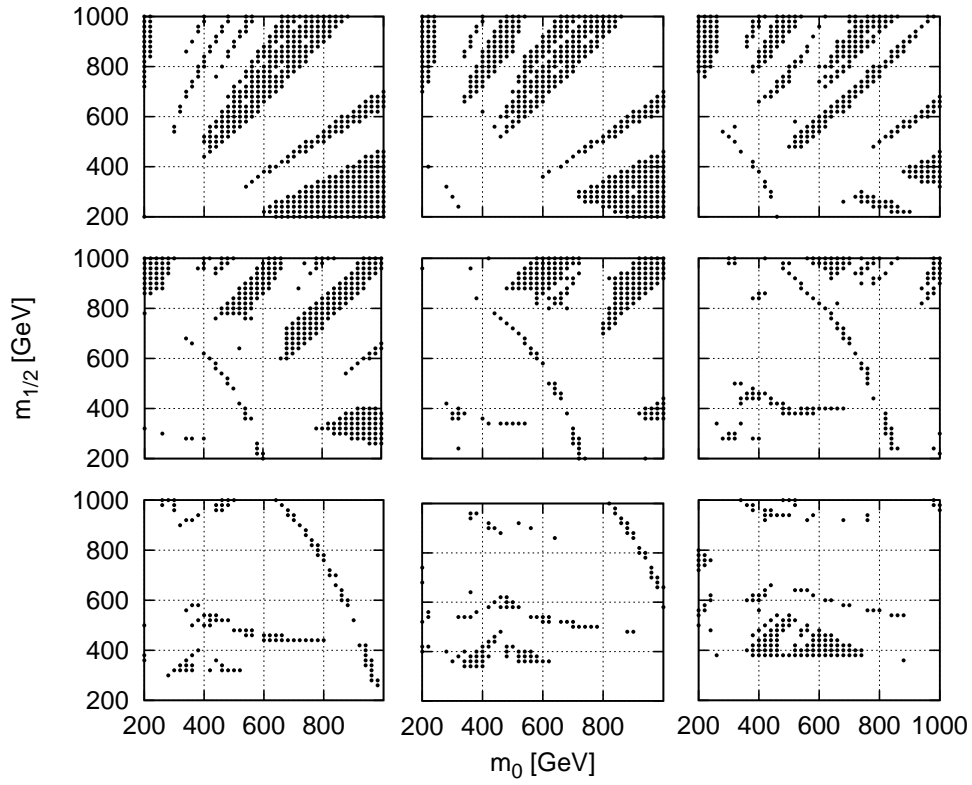


FIG. 7: Like Fig. 2 but for $\tan \beta = 30$.

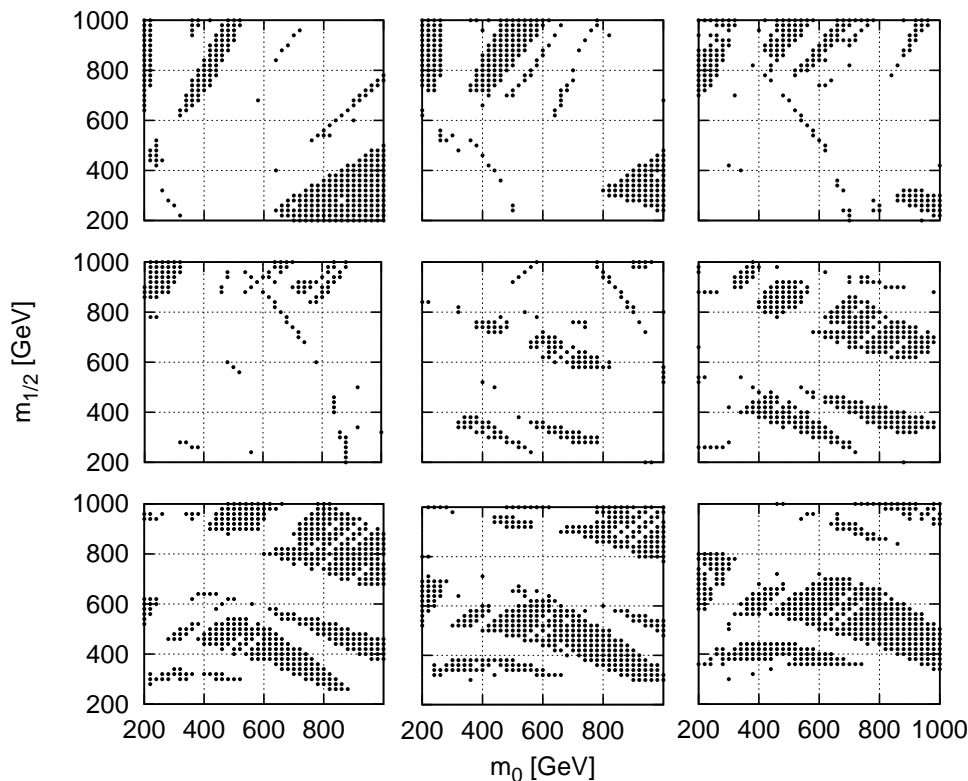


FIG. 8: Like Fig. 2 but for $\tan\beta = 35$.

the SUGRA benchmark points SPS1a, SPS1b, SPS2, and SPS3, are shown on Figs. 10–13. In this calculation we have not discriminated the results which were exceeding the upper limit for μ_ν .

The existing limits on Λ 's, obtained within SUSY models, oscillate around $10^{-2} - 10^{-5}$, depending on the method used [11, 35]. We check here the range between $\text{few} \times 10^{-2}$ and 10^{-10} . We notice that the RGE running decreases the values of Λ 's for higher energies [20], thus the parameter Λ_0 sets the upper limit on them.

We first notice, that below roughly $\Lambda_0 = 10^{-5}$ (in some cases even more) the results stabilize and do not change with decreasing Λ_0 , which makes them almost indistinguishable with the situation when all RpV couplings are set to zero. On the other hand, the calculations broke down for $\Lambda_0 > \text{few} \times 10^{-2}$. This leaves a rather narrow region of Λ_0 , between 1 and 3 orders of magnitude and only modestly exceeding 10^{-2} , for which the RpV couplings play a role.

We see also that for small Λ_0 the general alignment of the μ 's resembles hierarchical structure, while for high Λ_0 this hierarchy vanishes, and the results show no regular pattern. Too high values of Λ_0 can boost them to values close to $10^{-6} \mu_B$, which are excluded by experiments like MUNU [32] (recall upper limit from the MUNU $\sim 10^{-10} \mu_B$). Curiously, for small (or zero) values of Λ_0 , all the transition magnetic moments tend to be of the order of $10^{-10} \mu_B$ (SPS1a, SPS1b) or lower (SPS2,

SPS3).

Let us also compare the newly computed contributions with similar contributions coming from simplest loops with no mass insertions (trilinear RpV couplings only) and loops with bilinear insertions on the external neutrino lines (neutrino–neutralino mixing). We do it for two points, for which earlier calculations have been presented in Refs. [14, 16] – the unification with LOW values: $A_0 = 100$ GeV, $m_0 = m_{1/2} = 150$, and HIGH values: $A_0 = 500$ GeV, $m_0 = m_{1/2} = 1000$. In both of these cases $\tan\beta = 19$ and $\mu > 0$.

The results are shown in Tab. I for the LOW point and Tab. II for the HIGH unification point. Below the numerical values, results for pure trilinear loops [16] and bilinear contributions [14] are given as ranges, obtained for different cases (assumptions of the normal or inverted hierarchy of neutrino masses, data from the neutrinoless double beta decay searches).

For the LOW point the smallest contributions discussed in this paper are at least 5 orders of magnitude greater than any other calculated so far. This clearly shows, that the loops with heaviest particles (like higgsinos and charginos) tend to dominate the overall contribution to the magnetic moments. This result is not totally unexpected, but it was not fully clear, if the higher order process (amplitude proportional to four instead of two coupling constants) will not suppress the effect coming directly from the masses of the heavy particles. That

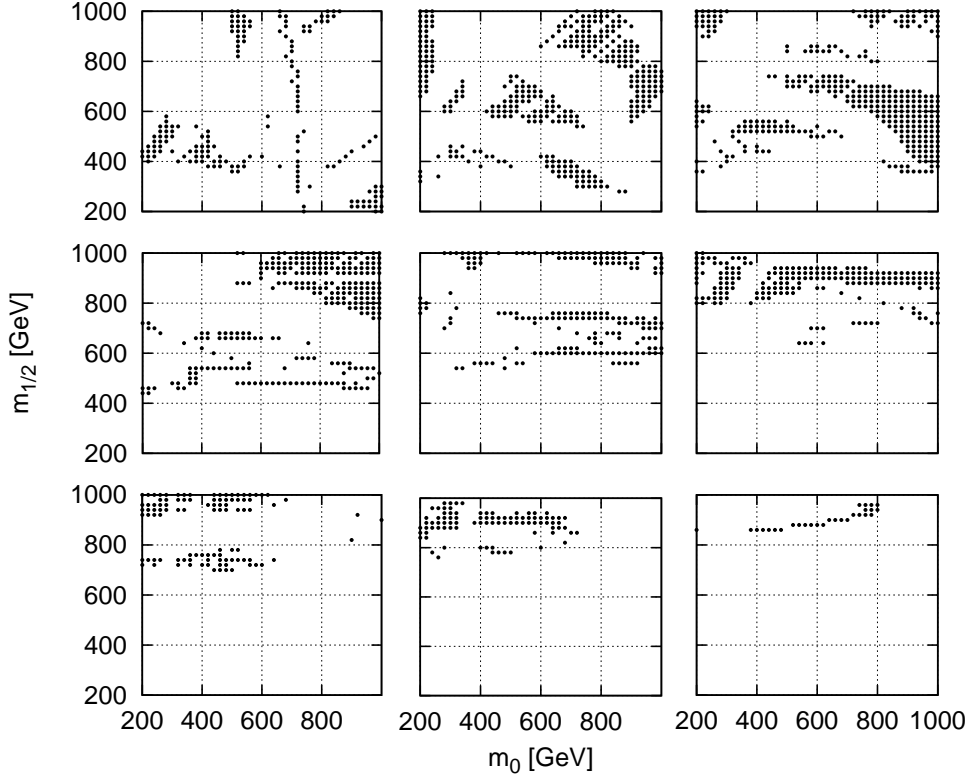


FIG. 9: Like Fig. 2 but for $\tan\beta = 40$. Please notice, that for such high value the model breaks down and the results are no longer reliable.

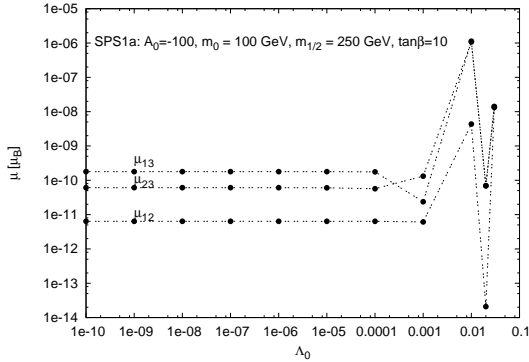


FIG. 10: Contributions to the magnetic moment of the neutrino for SPS1a SUGRA point.

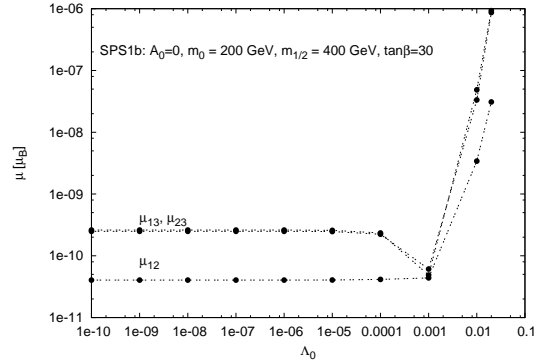


FIG. 11: Contributions to the magnetic moment of the neutrino for SPS1b SUGRA point.

VI. SUMMARY

was the case when the neutrino–neutralino mixing placed two mass insertions on the external neutrino lines of the diagrams. Here, however, the mass dependent loop functions \mathcal{I} are capable to boost the amplitudes of the process to very high values. All this holds also for the second, HIGH, set of input parameters, although there the difference between smallest value of $\mu_{\nu_{12}}$ and the maximum trilinear contribution is ‘only’ two orders of magnitude.

The full contribution to the Majorana neutrino transition magnetic moment consists of three main parts. The first one is represented by loop diagrams with two trilinear RpV couplings, containing either a quark–squark or lepton–slepton pair. The second takes into account possible neutrino–neutralino mixing, which occurs on the external neutrino lines in the form of bilinear mass insertions. The third one, discussed in this paper, allows for

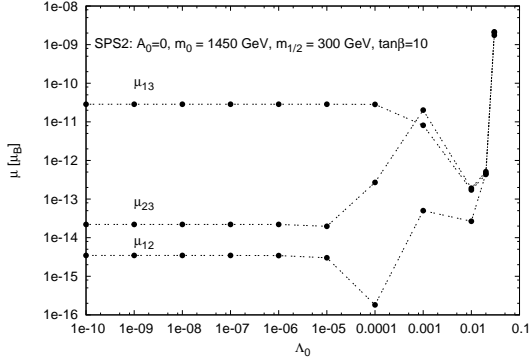


FIG. 12: Contributions to the magnetic moment of the neutrino for SPS2 SUGRA point.

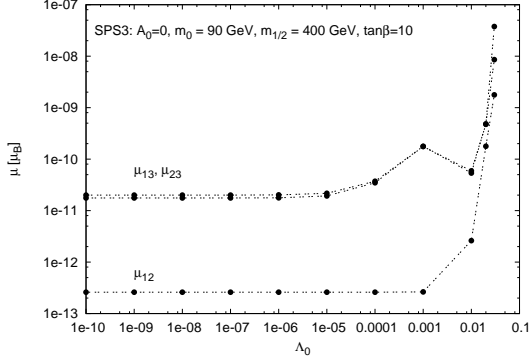


FIG. 13: Contributions to the magnetic moment of the neutrino for SPS3 SUGRA point.

the mass insertions to appear inside the loop, which may contain a number of different particles, i.e., charged Higgs bosons and the corresponding higgsinos, leptons and sleptons, charged gauge bosons, and charginos. A proper discussion of the latter contribution is possible only within a consistent R -parity violating model, in which all the mixing between different mass eigenstates is taken into account. Also, new terms in the RGE equations, proportional to the RpV couplings appear. However, the impact of these terms has already been studied [20] and their presence changed the low energy mass spectrum of the model by a factor of $1/5$ at most (20%). This indicates, that the crucial point is the phenomenon of mixing between different mass eigenstates, so that the amplitudes of the processes must be expanded in the physical bases and summed over respective eigenstates.

We have found that the presently discussed contributions are dominant over the remaining two. This allowed us to find the acceptable parameter space of the model, using the condition that no magnetic moment may exceed

$10^{-10} \mu_B$. We have also checked, how different initial values of the RpV couplings, represented by Λ_0 , change the results. Finally, a comparison with previous numerical studies has been given.

TABLE I: Comparison of the magnitudes of different contributions to the Majorana neutrino transition magnetic moments for the input parameters set LOW (see text). Here subscripts 1, 2, 3 = e, μ, τ .

Λ_0	$\mu_{\nu_{12}}$	$\mu_{\nu_{13}}$	$\mu_{\nu_{23}}$
3.0×10^{-2}	6.69×10^{-9}	3.21×10^{-7}	4.07×10^{-7}
2.0×10^{-2}	9.43×10^{-8}	1.41×10^{-7}	1.25×10^{-7}
1.0×10^{-2}	3.34×10^{-10}	2.40×10^{-9}	3.15×10^{-9}
1.0×10^{-3}	5.57×10^{-10}	2.09×10^{-7}	2.12×10^{-7}
1.0×10^{-4}	5.45×10^{-10}	4.97×10^{-8}	4.60×10^{-8}
1.0×10^{-5}	5.42×10^{-10}	4.61×10^{-8}	4.24×10^{-8}
1.0×10^{-6}	5.42×10^{-10}	4.58×10^{-8}	4.20×10^{-8}
1.0×10^{-7}	5.42×10^{-10}	4.58×10^{-8}	4.20×10^{-8}
1.0×10^{-8}	5.42×10^{-10}	4.58×10^{-8}	4.20×10^{-8}
1.0×10^{-9}	5.42×10^{-10}	4.58×10^{-8}	4.20×10^{-8}
1.0×10^{-10}	5.42×10^{-10}	4.58×10^{-8}	4.20×10^{-8}
trilinear	$10^{-19\dots-15}$	$10^{-19\dots-15}$	$10^{-18\dots-15}$
bilinear	$10^{-21\dots-17}$	$10^{-21\dots-17}$	$10^{-19\dots-17}$

TABLE II: Comparison of the magnitudes of different contributions to the Majorana neutrino transition magnetic moments for the input parameters set HIGH (see text). Here subscripts 1, 2, 3 = e, μ, τ .

Λ_0	$\mu_{\nu_{12}}$	$\mu_{\nu_{13}}$	$\mu_{\nu_{23}}$
3.0×10^{-2}	6.62×10^{-12}	2.66×10^{-9}	3.07×10^{-9}
2.0×10^{-2}	2.97×10^{-10}	1.34×10^{-10}	1.60×10^{-10}
1.0×10^{-2}	4.89×10^{-11}	2.19×10^{-10}	2.03×10^{-10}
1.0×10^{-3}	1.01×10^{-11}	3.75×10^{-7}	3.83×10^{-7}
1.0×10^{-4}	2.44×10^{-14}	8.02×10^{-9}	8.09×10^{-9}
1.0×10^{-5}	6.46×10^{-15}	4.32×10^{-9}	4.33×10^{-9}
1.0×10^{-6}	4.59×10^{-15}	4.05×10^{-9}	4.05×10^{-9}
1.0×10^{-7}	4.40×10^{-15}	4.02×10^{-9}	4.02×10^{-9}
1.0×10^{-8}	4.38×10^{-15}	4.02×10^{-9}	4.02×10^{-9}
1.0×10^{-9}	4.38×10^{-15}	4.02×10^{-9}	4.02×10^{-9}
1.0×10^{-10}	4.38×10^{-15}	4.02×10^{-9}	4.02×10^{-9}
trilinear	$10^{-20\dots-17}$	$10^{-20\dots-17}$	$10^{-20\dots-17}$
bilinear	$10^{-22\dots-18}$	$10^{-22\dots-18}$	$10^{-21\dots-18}$

Acknowledgments

This work has been financed by the Polish National Science Centre under the decision number DEC-2011/01/B/ST2/05932.

[1] G.L. Fogli *et al.*, Phys. Rev. D **78**, 033010 (2008).

[2] S. Fukuda *et al.* (Super-Kamiokande Collaboration),

- Phys. Rev. Lett. **81**, 1562 (1998); Y. Ashie *et al.* (Super-Kamiokande Collaboration), Phys. Rev. Lett. **93**, 101801 (2004); Phys. Rev. D **71**, 112005 (2005); T. Araki *et al.* (KamLAND Collaboration), Phys. Rev. Lett. **94**, 081801 (2005); Q.R. Ahmed *et al.* (SNO Collaboration), Phys. Rev. Lett. **87**, 071301 (2001); Phys. Rev. Lett. **89**, 011301 (2002); Phys. Rev. Lett. **89**, 011302 (2002); B. Aharmim *et al.* (SNO Collaboration), Phys. Rev. C **72** 055502 (2005); M. Apollonio *et al.* (CHOOZ Collaboration), Phys. Lett. B **466**, 415 (1999); Eur. Phys. J. C **27**, 331 (2003); G.L. Fogli, *et al.*, Phys. Rev. D **66**, 093008 (2002).
- [3] G. Altarelli, F. Feruglio, New J. Phys. **6**, 106 (2004), and references therein.
- [4] B. Kayser, Phys. Rev. D **26**, 1662 (1982).
- [5] J.F. Beacom, P. Vogel, Phys. Rev. Lett. **83**, 5222 (1999).
- [6] J. Schechter, J.W.F. Valle, Phys. Rev. D **25**, 774 (1982); G.B. Gelmini, J.W.F. Valle, Phys. Lett. B **142**, 181 (1984); M.C. Gonzalez-Garcia, J.W.F. Valle, Phys. Lett. B **216**, 360 (1989); J.F. Beacom, N.F. Bell, Phys. Rev. D **65**, 113009 (2002).
- [7] O. Haug, J.D. Vergados, A. Faessler, and S. Kovalenko, Nucl. Phys. B **565**, 38 (2000).
- [8] G. Bhattacharyya, H.V. Klapdor-Kleingrothaus, and H. Päs, Phys. Lett. B **463**, 77 (1999).
- [9] A. Abada, M. Losada, Phys. Lett. B **492**, 310 (2000); Nucl. Phys. B **585**, 45 (2000).
- [10] Y. Grossman, S. Rakshit, Phys. Rev. D **69**, 093002 (2004).
- [11] M. Gózdź, W.A. Kamiński, F. Šimkovic, Phys. Rev. D **70**, 095005 (2004).
- [12] M. Gózdź, W.A. Kamiński, F. Šimkovic, Int. J. Mod. Phys. E **15**, 441 (2006); Acta Phys. Polon. B **37**, 2203 (2006).
- [13] M. Gózdź, W. A. Kamiński, Int. J. Mod. Phys. E **17** (2008) 276.
- [14] M. Gózdź, W. A. Kamiński, Phys. Rev. D **78**, 075021 (2008).
- [15] S. Davidson, M. Losada, Phys. Rev. D **65**, 075025 (2002).
- [16] M. Gózdź, W.A. Kamiński, F. Šimkovic, A. Faessler, Phys. Rev. D **74** 055007 (2006).
- [17] M. Gózdź, W. A. Kamiński, Int. J. Mod. Phys. E **18**, 1094 (2009).
- [18] M. Gózdź, W. A. Kamiński, Phys. Rev. D **79**, 075023 (2009).
- [19] B.C. Allanach, A. Dedes, H.K. Dreiner, Phys. Rev. D **69**, 115002 (2004).
- [20] M. Gózdź, W. A. Kamiński, Phys. Rev. D **69**, 076005 (2004).
- [21] H.E. Haber, G.L. Kane, Phys. Rep. **117**, 75 (1985).
- [22] D.I. Kazakov, Beyond the Standard Model (In Search of Supersymmetry), lectures given at the European School on High Energy Physics, Caramulo (2000), and Schwarzwald Workshop, Bad Liebenzell (2000), hep-ph/0012288.
- [23] R. Barbier *et al.*, Phys. Rep. **420**, 1 (2005).
- [24] C. Aulakh, R. Mohapatra, Phys. Lett. B **119**, 136 (1982); G.G. Ross, J.W.F. Valle, Phys. Lett. B **151**, 375 (1985); J. Ellis *et al.*, Phys. Lett. B **150**, 142 (1985); A. Santamaria, J.W.F. Valle, Phys. Lett. B **195**, 423 (1987); Phys. Rev. D **39**, 1780 (1989); Phys. Rev. Lett. **60**, 397 (1988); A. Masiero, J.W.F. Valle, Phys. Lett. B **251**, 273 (1990).
- [25] M.A. Diaz, J.C. Romao, J.W.F. Valle, Nucl. Phys. B **524**, 23 (1998); A. Akeroyd *et al.*, Nucl. Phys. B **529**,3 (1998); A.S. Joshipura, M. Nowakowski, Phys. Rev. D **51**, 2421 (1995); Phys. Rev. D **51**, 5271 (1995).
- [26] M. Nowakowski, A. Pilaftsis, Nucl. Phys. B **461**, 19 (1996).
- [27] L.J. Hall, M. Suzuki, Nucl. Phys. B **231**, 419 (1984); G.G. Ross, J.W.F. Valle, Phys. Lett. B **151**, 375 (1985); R. Barbieri, D.E. Brahm, L.J. Hall, S.D. Hsu, Phys. Lett. B **238**, 86 (1990); J.C. Romao, J.W.F. Valle, Nucl. Phys. B **381**, 87 (1992); H. Dreiner, G.G. Ross, Nucl. Phys. B **410**, 188 (1993); D. Comelli *et al.*, Phys. Lett. B **324**, 397 (1994); G. Bhattacharyya, D. Choudhury, K. Sridhar, Phys. Lett. B **355**, 193 (1995); G. Bhattacharyya, A. Raychaudhuri, Phys. Lett. B **374**, 93 (1996); A.Y. Smirnov, F. Vissani, Phys. Lett. B **380**, 317 (1996); L.J. Hall, M. Suzuki, Nucl. Phys. B **231**, 419 (1984).
- [28] V. Barger, M.S. Berger, P. Ohmann, Phys. Rev. D **49**, 4908 (1994).
- [29] M. Beuthe, Phys. Rep. **375**, 105 (2003).
- [30] K. Nakamura *et al.* (Particle Data Group), J. Phys. G **37**, 075021 (2010).
- [31] O.G. Miranda, T.I. Rashba, A.I. Rez, J.W.F. Valle, Phys. Rev. Lett. **93**, 051304 (2004).
- [32] Z. Daraktchieva *et al.* (MUNU Collaboration), Phys. Lett. B **564**, 190 (2003); Phys. Lett. B **615**, 153 (2005).
- [33] The TEVNPH Working Group (CDF and D0 Collaborations), arXiv:1107.4960.
- [34] B.C. Allanach *et al.*, Eur. Phys. J. C **25**, 113 (2002).
- [35] K. Agashe, M. Graesser, Phys. Rev. D **54**, 4445 (1996); S. Chakrabarti, M. Guchait, N.K. Mondal, Phys. Lett. B **600**, 231 (2004); D.K. Ghosh, X.-G. He, B.H.J. McKellar, J.-Q. Shi, JHEP 0207:067, 2002; N. Yamanaka, T. Sato, T. Kubota, arXiv:1104.4533v1 [hep-ph]; ATLAS Collaboration, Eur. Phys. J. C **71**, 1809 (2011).